

# Optimization of Resistance Spot Welding Process Parameters on Shear Tensile Strength of SAE 1010 steel sheets Joint using Box-Behnken Design

Shashi Dwivedi<sup>a,b,\*</sup>, Satpal Sharma<sup>a</sup>

<sup>a</sup>School of Engineering, Gautam Buddha University, Greater Noida, Gautam Buddha Nagar, U.P. 201310, India

<sup>b</sup>Noida Institute of Engineering Technology, Greater Noida, Gautam buddha Nagar, U.P. 201310, India

Received 5 January 2014

Accepted 7 March 2016

## Abstract

In the present investigation, SAE 1010 steel sheets are welded by resistance spot welding. The welding current, welding cycle and electrode force are the principal variables that are controlled in order to provide the necessary combination of heat and pressure to form the weld. Response surface methodology (Box-Behnken Design) is chosen to design the experiments. In the range of process parameters, the result shows that as welding current increases shear tensile strength decreases, whereas welding time (cycle) and electrode force increase shear tensile strength increase. From the ANOVA table it can be concluded that electrode force is contributing more and it is followed by welding time and welding current. Optimum values of welding current (6 kA), welding time (25 cycle) and electrode force (4.5 kN) during welding of SAE 1010 steel sheets joint to maximize the shear tensile strength (Predicted 8.214 kN) have been find out. There was approximately 6.12 % error was found between experimental and modeled result.

© 2016 Jordan Journal of Mechanical and Industrial Engineering. All rights reserved

**Keywords:** Resistance spot welding, Box Behnken Design, SAE 1010 steel, Welding current, Shear Tensile strength.

## 1. Introduction

Resistance spot welding (RSW) has an important place in manufacturing and it is the simplest and most widely used form of the electric resistance welding processes in which faying surfaces are joined in one or more spots [1]. Spot welds are the dominant joining method in the automotive assembly process. As the automated assembly process is not perfect, some spot welds may be absent when the vehicle leaves the assembly line [2, 3].

Resistance Spot welding is a process in which contacting metal surfaces are joined by the heat obtained from resistance to electric current flow. Work-pieces are held together under pressure exerted by electrodes. Typically the sheets are in the 0.5 to 3 mm thickness range. The process uses two shaped copper alloy electrodes to concentrate welding current into a small "spot" and to simultaneously clamp the sheets together. The amount of heat (energy) delivered to the spot is determined by the resistance between the electrodes and the amperage and duration of the current. The amount of energy is chosen to match the sheet's material properties, its thickness, and type of electrodes. Applying too little energy won't melt the metal or will make a poor weld [4].

Applying too much energy will melt too much metal, eject molten material, and make a hole rather than a weld. Another attractive feature of spot welding is the energy delivered to the spot can be controlled to produce reliable welds [5,6].

M. Pouranvari [7] *et al.* in 2011 investigated the effect of the welding parameters (welding time, welding current and electrode force) on the overload failure mode and mechanical performance of dissimilar resistance spot welds between drawing quality special killed AISI 1008 low carbon steel and DP600 dual phase steel. Mechanical properties of spot welds are described in terms of failure mode, peak load and energy absorption during the quasi-static tensile-shear test. Three distinct failure modes were observed during the tensile-shear test: interfacial, pullout and partial thickness-partial pullout failure modes. Correlations among failure mode, welding parameters, weld physical attributes and weld mechanical performance are analyzed. Effect of expulsion on mechanical performance of welds is also investigated.

In Sung Hwang [8] *et al.* in 2011 studied on expulsion reduction in resistance spot welding by controlling of welding current waveform and discussed on welding problem such as expulsion in resistance spot welding of high strength steel.

\* Corresponding author e-mail: shashi\_gla47@rediffmail.com.

R.S. Florea [9] *et al.* in 2012 welded 6061-T6 aluminum by resistance spot welding and for characterization. Electron Back Scatter Diffraction (EBSD) scanning, tensile testing, Laser Beam Profilometry (LBP) measurements along with optical microscopy (OM) images, failure loads and deformation of 6061-T6 aluminum alloy were experimentally investigated of resistance spot welding.

Hessamoddin Moshayedi [10] *et al.* in 2012 studied on nugget size growth in resistance spot welding of austenitic stainless steels and developed A 2D axisymmetric electro-thermo-mechanical Finite Element (FE) model is to study the effect of welding time and current intensity on nugget size in resistance spot welding process of AISI type 304L austenitic stainless steel sheets using ANSYS commercial software package.

Shear tensile strength plays a key role in determining the welding strength of the weld plates SAE1010 steel sheets. Shear strength is the strength of a material or component against the type of yield or structural failure where the material or component fails in shear. A shear load is a force that tends to produce a sliding failure on a material along a plane that is parallel to the direction of the force. Welding of sheets by resistance spot welding is dependent on many factors, it is more influenced by parameters like welding current, welding time and electrode force. In the present investigation, response surface methodology (Box-Behnken Design) used to determine the welding process parameters with the optimal shear tensile strength are investigated [11].

## 2. Materials and Methods

### 2.1. Workpiece Material

The present work was planned to optimize the resistance spot welding parameters of SAE 1010 steel sheets with constant thicknesses. The specimens were prepared by cutting the workpiece material into the

suitable dimensions and then cleaned and abraded to prevent high contact resistance which is created due to an oxide layer. The tensile shear test experiments were performed on the specimens according to welding standards of the Resistance Welders Manufacturer Association (RWMA). SAE 1010 steel is used for applications such as cold headed fasteners and bolts, Tubular Products, Bar Products, Wire Products, Fasteners, and Piping Components. The chemical composition (percent by weight), and the mechanical properties of the SAE 1010 steel sheet are given in Table 1 and Table 2, respectively. The dimensions of the specimens used throughout the experiment are also given in Table 3 [12].

**Table 1.** Chemical composition of SAE 1010 steel sheet[13]

| Percent Composition | C     | Mn   | Si   | P     | S     |
|---------------------|-------|------|------|-------|-------|
|                     | 0.082 | 0.62 | 0.18 | 0.013 | 0.016 |

**Table 2.** Mechanical properties of SAE 1010 steel sheet[13]

| Mechanical Properties | Yield Strength | Tensile Strength | % Elongation | Hardness (HB) |
|-----------------------|----------------|------------------|--------------|---------------|
|                       | 327            | 418              | 33.5         | 78            |

**Table 3.** Dimensions of the workpieces

| Thickness (t) (mm) | Width (W) (mm) | Length (L) (mm) | Contact Overlap (mm) |
|--------------------|----------------|-----------------|----------------------|
| 2                  | 25.4           | 101.6           | 25.4                 |

### 2.2. Electrode Material

Copper was used as an electrode material and it was reserved constant during all the seventeen experiments. The electrode was changed with a non-used one for each experiment run to prevent the effect of electrode damage on the nugget formed. Copper electrode dimension, electrode before using and after using are shown in Figure 1 (a), (b) and (c), respectively.

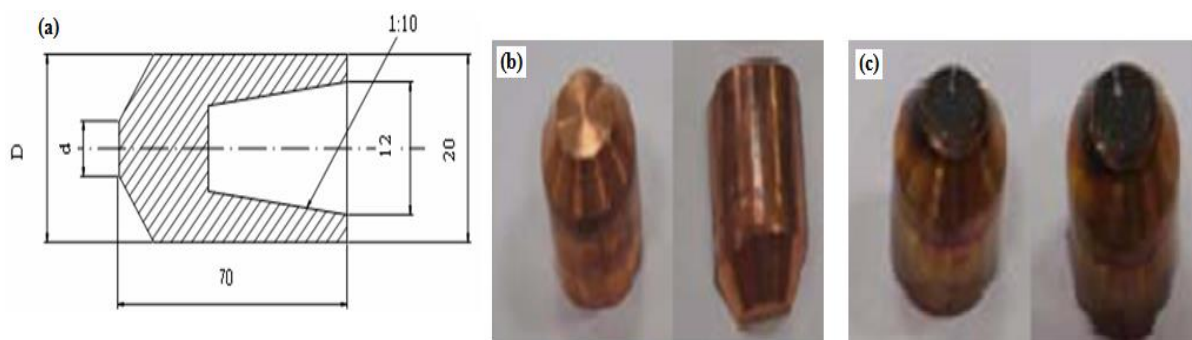


**Figure 1.** Electrode material (a) Copper electrode dimension (b) electrode before using (c) electrode after using

2.3. Experimental Procedure

A Resistance spot welding machine was used for resistance spot welding of SAE 1010 steel sheets with constant thickness 2 mm. The required sensors are placed in relevant positions for most effective detection as shown in Figure 2. The current sensor (not visible) is a Rogowski (air cored) coil. This sensor gives a voltage output proportional to the current induced through the arms of the spot weld machine. The voltage sensor consists of two leads connected to each copper electrode.

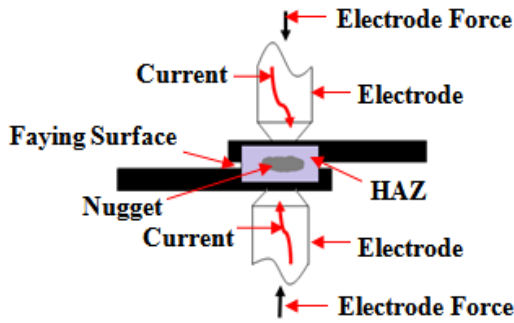


Figure 2. Resistance spot welding process

There are various process parameters of resistance spot welding machine affecting the resistance spot welding characteristics. On the basis of pilot investigations, the following process parameters have been selected for study. Their ranges are given in Table 4.

Table 4. Resistance spot welding process parameters with their ranges

| S.No. | Input parameters     | Ranges  |
|-------|----------------------|---------|
| 1     | Current (kA)         | 6 -10   |
| 2     | Welding time (Cycle) | 15 -25  |
| 3     | Electrode force (KN) | 1.5-4.5 |

Welding of SAE 1010 steel sheet was carried out by resistance spot welding as per the plan of experiments tabulated in Table 5 and measured shear tensile strength measured on tensometer tensile testing machine are also given in Table 5.

2.4. Response Surface Methodology

The response surface methodology is used to design the experiment for the given problem. In this study, three parameters are used as levels that maximize the yield (y) of a process [14]. The process yield is a function of the different constituents, say

$$y = f(x_1, x_2, x_3) + \epsilon \tag{1}$$

where  $\epsilon$  represents the noise or error observed in the response y. if we denote the expected response (tensile strength) by  $E(y) = f(x_1, x_2, x_3, x_4, x_5) = \eta$ , then the response represented [15] by

$$\eta = f(x_1, x_2, x_3) \tag{2}$$

is called a response [16].

Box-Behnken design is used to further study the quadratic effect of factors after identifying the significant factors using screening factorial experiments [17-19].

Table 5. Design matrix and experimental results

| Standard Order | Current (kA) | Welding Time (Cycle) | Electrode Force (kN) | Shear Tensile Strength (MPa) |
|----------------|--------------|----------------------|----------------------|------------------------------|
| 1              | 10           | 20                   | 1.5                  | 7.3                          |
| 2              | 8            | 15                   | 4.5                  | 8.1                          |
| 3              | 8            | 25                   | 1.5                  | 7.5                          |
| 4              | 8            | 15                   | 1.5                  | 7.2                          |
| 5              | 8            | 25                   | 4.5                  | 9.4                          |
| 6              | 8            | 20                   | 3                    | 8.2                          |
| 7              | 10           | 15                   | 3                    | 7.7                          |
| 8              | 8            | 20                   | 3                    | 8.15                         |
| 9              | 8            | 20                   | 3                    | 8.2                          |
| 10             | 6            | 15                   | 3                    | 8.7                          |
| 11             | 6            | 25                   | 3                    | 9.4                          |
| 12             | 10           | 20                   | 4.5                  | 8.3                          |
| 13             | 10           | 25                   | 3                    | 8.8                          |
| 14             | 6            | 20                   | 1.5                  | 8                            |
| 15             | 8            | 20                   | 3                    | 8.27                         |
| 16             | 8            | 20                   | 3                    | 8.25                         |
| 17             | 6            | 20                   | 4.5                  | 9.4                          |

3. Results and Discussion

3.1. Macrographic View of SAE 1010 Steel Sheet Joint

Figure 3 shows several macrographic views of the nugget of SAE 1010 steel sheet joint, welded by resistance spot welding in the range of process parameters. The macrographic examinations are carried out to find out the shape of the nuggets. Unbalance heat (beyond the range of process parameters) causes irregular nugget formation (Figure 3 (g)). The weld nugget loses its symmetric form because of the uneven heat ensuing from different physical properties of the steel sheets (SAE 1010 steel sheets). The nugget formation is more active in stainless steel sheet, since stainless steel has a higher electrical resistance. Each macrographic view shows that SAE 1010 steel sheets are fully melted, but sometimes undesired effect is occurred when welding is done at high current as shown in Figure 3(g).

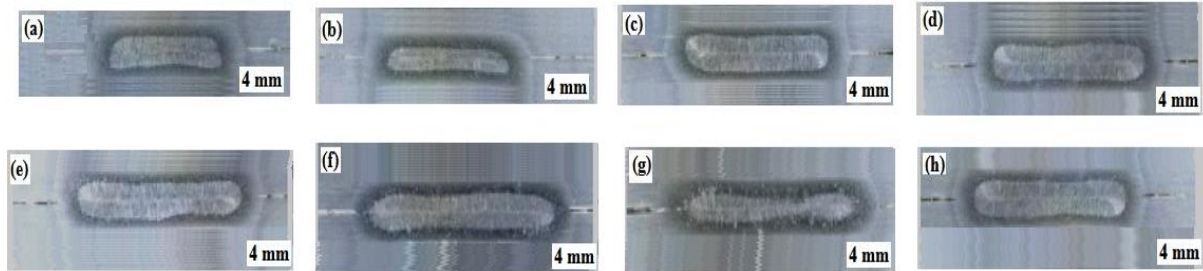


Figure 3: Macrographic views of resistance spot welded joint of SAE 1010 steel sheet at welding current of 6 kA, welding time of 25 cycles and electrode force of 4.5 kN

### 3.2. Micrographic View of SAE 1010 Steel Sheet Joint

Figure 4 presents the micrographic views of the welded specimens joined at various welding current, welding time and electrode forces (in the range of process parameters). It can be seen from Figure 4 that difference in terms of color is identified among the grains due to intergranular direction. Crack and porosity were also not observed around the weld region.

### 3.3. Microstructure Analysis of Welded Joint and HAZ

To examine the microstructure of the weld SAE 1010 steel sheet and heat affected zones, the microstructure analysis was carried out. Figure 5 displays the microstructures of the SAE 1010 steel sheet, weld joint and heat affected zones. Development of grain was observed in SAE 1010 steel sheet and welded joint. Columnar structures were identified in weld nugget zone.

### 3.4. Analysis of Shear Tensile Strength

The preferred experimental design is box behnken design and the design matrix is exposed in Table 5. The analysis of response was done via design expert software. Analysis of variance for tensile strength is given in Table 6. Values of "Prob>F" are less than 0.0500 point out that model terms are significant. From the Table 6, linear terms welding current, welding time, electrode force, square terms of welding current, welding time, electrode force and interaction terms between parameters are significant model terms. Values greater than 0.10 show that model terms are not significant. The final empirical relationship was constructed using only these coefficients, and the developed final empirical relationship is given below:

$$\begin{aligned} \text{Tensile Shear Strength} = & +15.56200 - 1.58450 * \\ & \text{Current} - 0.28380 * \text{Welding Time} + 0.78533 * \\ & \text{Electrode Force} + 1.00000\text{E-}002 * \text{Current} * \\ & \text{Welding Time} - 0.033333 * \text{Current} * \\ & \text{Electrode Force} + 0.033333 * \text{Welding Time} * \\ & \text{Electrode Force} + 0.079500 * \text{Current}^2 + \\ & 4.72000\text{E-}003 * \text{Welding Time}^2 - 0.12533 * \\ & \text{Electrode Force}^2 \end{aligned} \quad (3)$$

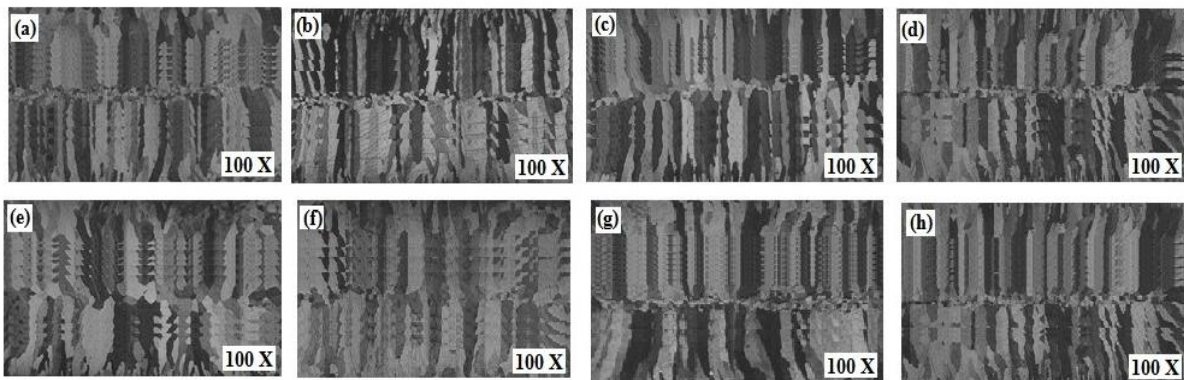


**Figure 4:** Micrographic views of resistance spot welded joint of SAE 1010 steel sheet at welding current of 6 kA, welding time of 25 cycles and electrode force of 4.5 kN

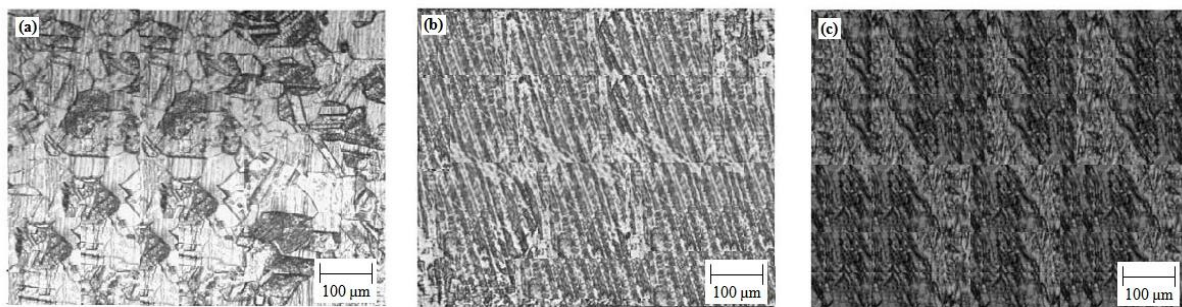


**Figure 5:** Microstructure of (a) SAE 1010 steel sheet, (b) welded joint, (c) HAZ



**Table 6:** Analysis of variance (ANOVA) for shear tensile strength

| Source         | Sum of Square | DF    | Mean Square | F value        | Prob.>F  |                 |
|----------------|---------------|-------|-------------|----------------|----------|-----------------|
| Model          | 7.38          | 9     | 0.82        | 147.56         | < 0.0001 | Significant     |
| A              | 1.44          | 1     | 1.44        | 259.89         | < 0.0001 |                 |
| B              | 1.45          | 1     | 1.45        | 259.89         | < 0.0001 |                 |
| C              | 3.38          | 1     | 3.38        | 607.91         | < 0.0001 |                 |
| AB             | 0.04          | 1     | 0.04        | 7.19           | 0.0314   |                 |
| AC             | 0.04          | 1     | 0.04        | 7.19           | 0.0314   |                 |
| BC             | 0.25          | 1     | 0.25        | 44.96          | 0.0003   |                 |
| A <sup>2</sup> | 0.43          | 1     | 0.43        | 76.58          | < 0.0001 |                 |
| B <sup>2</sup> | 0.059         | 1     | 0.059       | 10.54          | 0.0141   |                 |
| C <sup>2</sup> | 0.33          | 1     | 0.33        | 60.22          | 0.0001   |                 |
| Residual       | 0.039         | 7     | 5.560E-003  |                |          | Not Significant |
| Lack of Fit    | 0.030         | 3     | 0.010       | 4.48           | 0.0906   |                 |
| Pure Error     | 8.92E-003     | 4     | 2.23E-003   |                |          |                 |
| Cor Total      | 7.42          | 16    |             |                |          |                 |
| Std. Dev.      |               | 0.075 |             | R-Squared      |          | 0.9948          |
| Mean           |               | 8.29  |             | Adj R-Squared  |          | 0.9880          |
| C.V. %         |               | 0.90  |             | Pred R-Squared |          | 0.9335          |
| PRESS          |               | 0.49  |             | Adeq Precision |          | 38.469          |

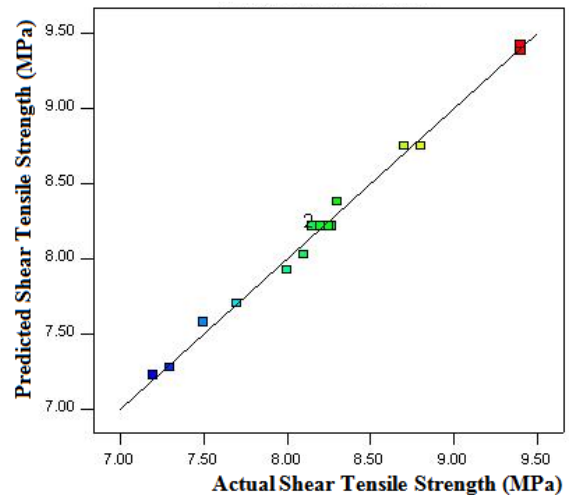
Analysis of variance (ANOVA) method was used to check the adequacy of the developed empirical correlation. In the present work, the preferred level of confidence was measured to be 95%. The model F value of 147.56 reveals that the model is significant. There is only a 0.01% possibility that a model F value this large could take place due to noise. The lack of fit F value of 4.48 indicates that the lack of fit is insignificant. There is only a 9.06% possibility that a lack of fit F value this large could occur due to noise.

The rightness of fit of the model was checked by the determination coefficient ( $R^2$ ). The coefficient of determination ( $R^2$ ) was calculated to be 0.9948 for response (shear tensile strength). This indicates that 99.48% of experimental data confirms the compatibility with the data predicted by the model. The  $R^2$  value is always between 0 and 1, and its value indicates exactness of the model. For a good statistical model,  $R^2$  value should be close to 1.0. The adjusted  $R^2$  value reconstructs the appearance with the significant terms.

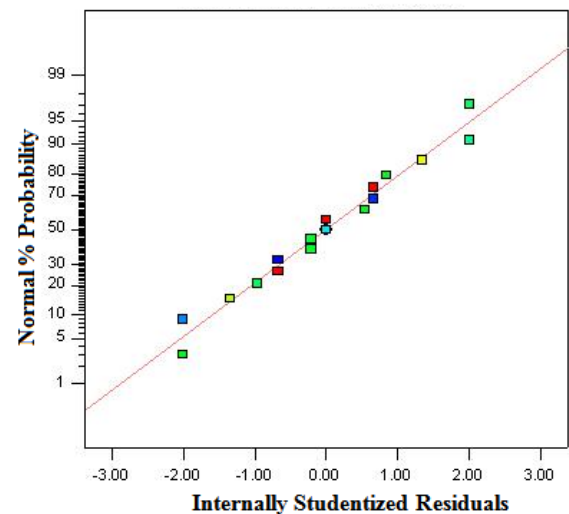
Figure 6 displays the relationship between the predicted and experimental values for shear tensile strength. After the regression model of shear tensile strength was developed, the model adequacy examination was performed in order to validate that the essential assumption of regression analysis is not violated.

Figure 7 shows the normal probability plot of the residual which shows no sign of the violation since each point in the plot follows a straight line pattern. The normal probability plot is used to validate the normality assumption. The data are spread approximately along the straight line. Hence, it is concluded that the data are normally distributed.

The influence of resistance spot welding process parameters like welding current, welding time, electrode force, were evaluated against shear tensile strength of welded shear tensile pieces SAE1010. Figures 8 to 10 show the interaction effect of welding current, welding time and electrode force on shear tensile strength.



**Figure 6:** Correlation between the predicted and actual values of tensile strength in MPa



**Figure 7:** The normal probability of residuals

3.4.1. The Effect of Welding Current on Shear Tensile Strength

Figures 8 and 9 show the effect of welding current on the shear tensile strength of welds indicating that that generally increasing welding current, decreases the shear tensile strength. When the current is passed through the electrodes to the sheets, heat is generated, resulting in a

higher electrical resistance produced at the surface contact of SAE 1010 steel sheets. Electrical resistance of the material produces heat between the work pieces and the copper electrodes, the rising heat causes a rising temperature, and results in a molten pool contained most of the time between the electrodes.

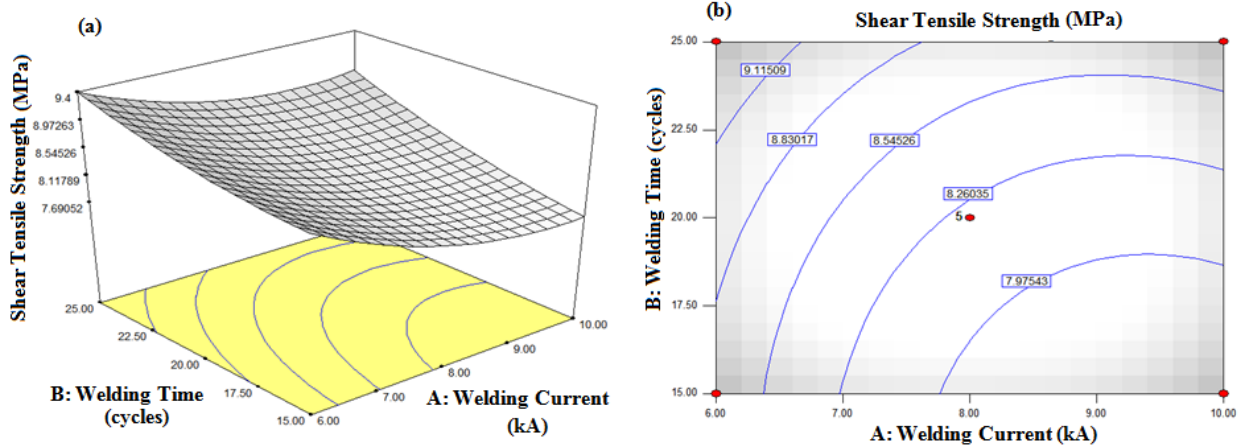


Figure 8: Interaction effect of welding current and welding time on shear tensile strength. (a) 3D interaction (b) the contour plot.

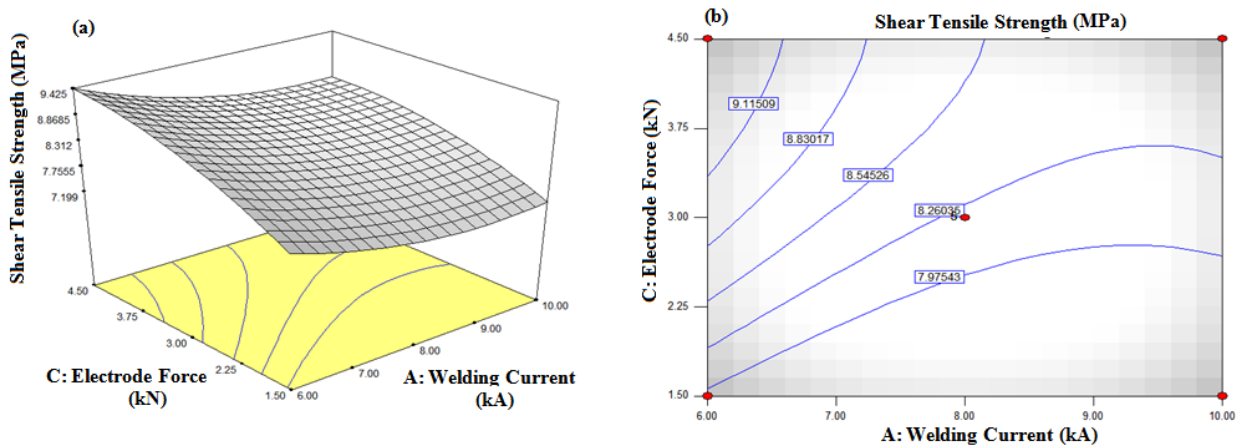


Figure 9: Interaction effect of welding current and electrode force on shear tensile strength. (a) 3D interaction (b) the contour plot

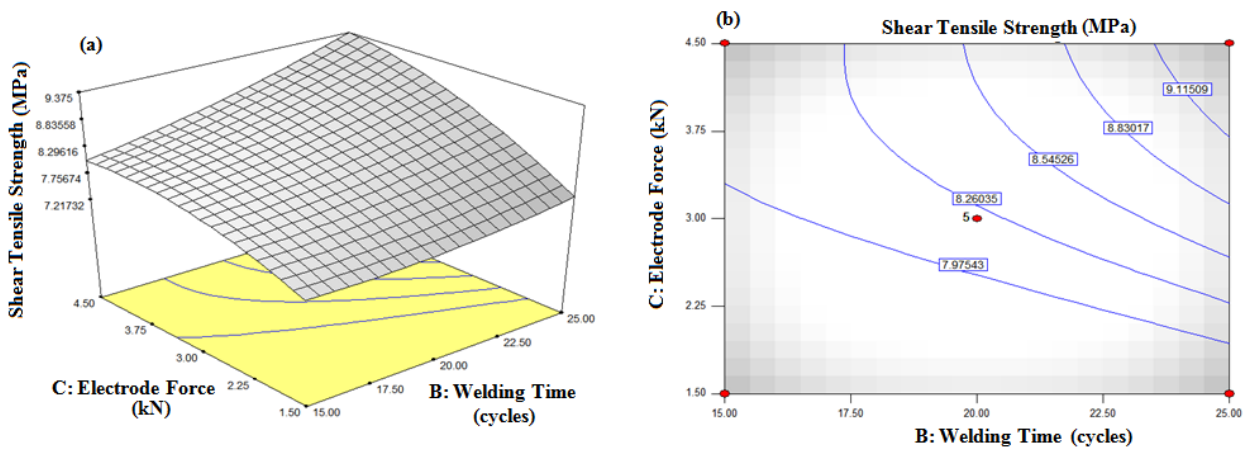


Figure 10: Interaction effect of welding time and electrode force on shear tensile strength. (a) 3D interaction (b) the contour plot

### 3.4.2. The Effect of Welding Time on Shear Tensile Strength

As seen in Figures 8 and 10, welding time (cycle) increases from minimum to maximum limit, the shear tensile strength also increases. When the heat dissipates throughout the workpiece in less time (resistance welding time is generally programmed as cycles), the molten or plastic state grows to meet the welding tips. When the current is stopped, the copper tips cool the spot weld, resulting the metal solidified under pressure.

### 3.4.3. The Effect of Electrode Force on Shear Tensile Strength

In experimental studies shown in Figures 9 and 10, tensile strength increased while electrode force increased because if the electrode force between the base materials is low, then the molten area may extend to the exterior of the work pieces, escaping the containment force of the electrodes. This burst of molten metal is called expulsion, and when this occurs the metal will be thinner and have less shear strength.

### 3.5. Confirmation Experiment

The optimum parameters that give up the maximum shear tensile strength are welding current of 6 kA, welding time of 25 cycles and electrode force 4.5 kN. Importance of process parameters can be ranked from their F ratio which is mentioned in Table 6. . It can be concluded that electrode force is contributing more and it is followed by welding time and welding current. At the 95% PI low value was found 8.020 MPa, while at 95% PI high value was found 8.4071 kN. The average achievable predicted shear tensile strength is found to be 8.214 MPa. The experimental shear tensile strength (average of three test samples) corresponding to these parameters (welding current of 6 kA, welding time of 25 cycles and electrode force 4.5 kN) was found to be 8.75 MPa. This shows that there is approximately 6.12 % error in the experimental and modeled results. Hence, the developed model can be effectively used in the process parameter range to predict the shear tensile strength of resistance spot welded joint.

## 4. Conclusions

The following conclusions can be drawn from analysis:

1. The resistance spot welding process was found to be successful to weld SAE 1010 steel sheets. In the range of resistance spot welding process parameters, macrographic view, micrographic view and microstructure of the welded joint showed proper fusion of base materials (SAE 1010 steel sheets) and very less amount of crack and porosity was observed.
2. Based on analysis of variance (ANOVA), welding current, welding time (cycle), and electrode force were found to be significant factors. Interactions of parameters were also found significant interactions. The response surface methodology was used effectively to model the shear tensile strength of resistance spot welded joint. Within the resistance spot welding process parameters range, the shear tensile strength of SAE 1010 steel sheets joint decreases with the increase

in welding current while shear tensile strength increases with the increase in welding time (cycle) and electrode force from minimum to maximum limit.

3. Within the resistance spot welding process parameters the optimum parameters for shear tensile strength was found to be lower welding current (6 kA), higher welding time (25 cycles), and higher electrode force (4.5 kN). The predicted value of shear tensile strength was found 8.214 MPa at 95% confidence interval. There is approximately 6.12 % error in the experimental and modeled results.

## References

- [1] B.H. Chang, Y. Zhou, "Numerical study on the effect of electrode force in small-scale resistance spot welding". *Journal of Materials Processing Technology*, Vol. 139, No. 3, 2003, 635-641.
- [2] Jiang Xu Jianhui, Zeng, Qiang Xiuping, "Optimization of resistance spot welding on the assembly of refractory alloy 50Mo-50Re thin sheet". *Journal of Nuclear Materials*, Vol. 366, No. 3, 2007, 417-425.
- [3] Zhao Zou Jiasheng, Zheng Chen Qizhang, "Surface modified long-life electrode for resistancespotwelding of Zn-coated steel". *Journal of Materials Processing Technology*, Vol. 8, 2009, 4141-4146.
- [4] Hongxin Shi, Ranfeng Qiu, Jinhong Zhu, "Effects of welding parameters on the characteristics of magnesium alloy joint welded by resistance spot welding with cover plates". *Materials & Design*, Vol. 31, No. 10, 2010, 4853-4857.
- [5] Ramin Hashemi, Hamed Pashazadeh, Mohsen Hamed, "An Incrementally Coupled Thermo-Electro-Mechanical Model for Resistance Spot Welding". *Materials and Manufacturing Processes*, Vol. 27, No. 12, 2012, 1442-1449.
- [6] Ranfeng Qiu, Hongxin Shi, Hua Yu, Keke Zhang, Yimin Tu, S Satonaka, "Effects of Electrode Force on the Characteristic of Magnesium Alloy Joint Welded by Resistance Spot Welding with Cover Plates". *Materials and Manufacturing Processes*, Vol. 25, No. 11, 2010, 1304-1308.
- [7] M. Pouranvari, S.M. Mousavizadeh, S.P.H. Marashi, "Influence of fusion zone size and failure mode on mechanical performance of dissimilar resistance spot welds of AISI 1008 low carbon steel and DP600 advanced high strength steel". *Materials & Design*, Vol. 32, No. 3, 2011, 1390-1398.
- [8] In Sung Hwang, Mun Jin Kang, Dong Cheol Kim, "Expulsion Reduction in Resistance Spot Welding by Controlling of welding Current Waveform". *Procedia Engineering*, Vol. 10, 2011, 2775- 2781.
- [9] R.S. Florea, K.N. Solanki, "Resistance spot welding of 6061-T6 aluminum: Failure loads and deformation". *Materials & Design*, Vol. 34, 2012, 624-630.
- [10] Hessamoddin Moshayedi, Iradj Sattari-Far, "Numerical and experimental study of nugget size growth in resistance spot welding of austenitic stainless steels". *Journal of Materials Processing Technology*, Vol. 212, No. 2, 2012, 347-354.
- [11] S. M. Darwish, S. D. Al-Dekhial, "The Response Surface Approach to Spot Welding Commercial Aluminum Sheets". *Materials and Manufacturing Processes*, Vol. 13, No. 2, 1998, 189-202.
- [12] G. Biilir Omer, "The relationship between the parameters C and n of Paris' law for fatigue crack growth in SAE 1010 steel". *Engineering Fracture Mechanics*, Vol. 36, No.2, 1990, 361-364.
- [13] M.T. Yu, D.L. Du Quesnay, T.H. Topper, "Deformation and fatigue behaviour of cold-rolled SAE 1010 steel". *International Journal of Fatigue*, Vol. 12, No. 5, 1990, 433-439.

- [14] Montgomery Douglas C, "Design and Analysis of Experiments". Wiley-India, 2007, 5<sup>th</sup> edition: 427.
- [15] V. Balasubramanian, A. K. Lakshminarayanan, R. Varahamoorthy, S. Babu, "Understanding the Parameters Controlling Plasma Transferred Arc Hardfacing Using Response Surface Methodology". Materials and Manufacturing Processes, Vol. 23, No. 7, 2008, 674-682.
- [16] T. Kim, H. Park, S Rhee, "Optimization of welding parameters for resistance spot welding of TRIP steel with response surface methodology". International Journal of Production Research, Vol. 43, No. 21, 2005, 4643-4657.
- [17] Dipayan Das, B. S. Butola, S. Renuka, "Optimization of Fiber-Water Dispersion Process Using Box-Behnken Design of Experiments Coupled with Response Surface Methodology of Analysis". Journal of Dispersion Science and Technology, Vol. 33, No. 8, 2012, 1116-1120.
- [18] S. P. Dwivedi, "Effect of process parameters on tensile strength of friction stir welding A356/C355 aluminium alloys joint". Journal of Mechanical Science and Technology, Vol. 28, No. 1, 2014, 285-291.
- [19] S. P. Dwivedi, S. Sharma, "Effect of Process Parameters on Tensile Strength of 1018 Mild Steel Joints Fabricated by Microwave Welding". Metallogr. Microstruct. Anal., Vol. 3, 2014, 58-69.
- [20] S. P. Dwivedi, S. Sharma and R. K. Mishra, "Microstructure and mechanical behavior of A356/SiC/Fly-ash hybrid composites produced by electromagnetic stir casting" J Braz. Soc. Mech. Sci. Eng., Vol. 37, 2015, 57-67.